Advances in Science and Technology Research Journal

Advances in Science and Technology Research Journal 2022, 16(3), 111–123
https://doi.org/10.12913/22998624/149369
ISSN 2299-8624, License CC-BY 4.0

Received: 2022.02.05
Accepted: 2022.04.21
Published: 2022.05.15

Internal Corrosion Damage Mechanisms of the Underground Water Pipelines

Desalegn A. Yeshanew[1], Moera G. Jiru[1], Hirpa G. Lemu[2*], Mesay A. Tolcha[3]

[1] Department of Mechanical Engineering, Adama Science and Technology University, Ethiopia
[2] Faculty of Science and Technology, University of Stavanger, 4036 Stavanger, P.O. Box 8600, Norway
[3] Faculty of Mechanical Engineering, Jimma University, Ethiopia
* Corresponding author's e-mail: hirpa.g.lemu@uis.no

ABSTRACT

Internal water pipe corrosion is a complicated problem due to the interaction of water quality parameters with the pipe wall. This study presents investigations of internal pipe surface corrosion mechanisms related to water physicochemical. Samples of water and corrosion-damaged ductile cast iron (30+ years) and galvanized steel pipe (15–20 years) were collected under in-situ condition from Addis Ababa city water distribution system. Scanning electron microscopy and optical microscopy were used to examine the pipes' corrosion morphology and microstructures, respectively. Additionally, Mountains 9 surface analysis software was used for further pitting corrosion characterization.To identify the causes of internal pipe corrosion, water physicochemical analyses were conducted by using inoLab pH 7310P, DR 900, Palintest Photometer 7100, and Miero 800. Water physicochemical test indicates: $CaCO_3$ is 77–215 ppm, pH is 7.05 – 7.86, total dissolved solids (TDS) is 84.10–262.8 ppm, ClO_2 is 0–0.5 ppm, and dissolved oxygen (80–81 ppb). From water test results, major causes of internal pipe corrosion damage mechanisms were identified as dissolved oxygen, $CaCO_3$, TDS, ClO_2, and resistivity of water which initiates a differential cell that accelerates pipe corrosion. Using Mountain 9 surface analysis software, corrosion morphology and pitting features were characterized. The outputs of this paper will be helpful for water distribution and buried infrastructure owners to investigate corrosion damage mechanisms at an early stage. To manage corrosion mechanisms, water supply owners need to conduct frequent inspections, recording of pipe data, testing of water quality, periodic pipelines washing, and apply preventative maintenance.

Keywords: internal corrosion; water pipes; water physicochemical; corrosion mechanisms.

INTRODUCTION

Ferrous materials are widely used for different industrial product applications due to their versatility and mechanical properties. Despite being used for a variety of purposes, these materials are vulnerable to corrosion, which weakens the physical, chemical, and mechanical properties of metallic materials while in service. Internal corrosion is the time-dependent and slow degradation of metals induced by an electrochemical reaction [1, 2]. Internal pipes corrosion and the formation of deposits on the pipe walls are influenced by water quality parameters [3]. Different forms of internal corrosion can attack water pipe walls including uniform corrosion, localized corrosion, stress corrosion cracking (SCC), erosion-corrosion, and crevice corrosion. Corrosion forms variety of scales on the surface of metallic materials including goethite (α-FeOOH), magnetite (Fe_3O_4), and lepidocrocite (γ-FeOOH) [4]. Corrosion, on the other hand, can influence water quality as a result of interactions with heavy metal traces such as Cu, Mn, Ni, Pb, Cr, and arsenic that have collected inside water [5]. Furthermore, pipeline deterioration and collapse are influenced by a variety of elements, including the environment, pipe material, and operational service, all of which contribute to pipeline damage [6].

Uniform and localized corrosions are the two common types of pipe corrosion damage that cause failure before the expected service life [7, 8]. As deposition and trace elements increase in the water pipe, the wall becomes more deteriorated during the stagnant condition of water flow [9]. Internal corrosion scales are made up of several crystalline phases, including α-FeOOH, Fe_3O_4, and γ-FeOOH tend to be dominant, while siderite ($FeCO_3$), and hematite (Fe_2O_3) are frequently found as scales [10, 11]. Samples from real-world pipe distribution systems, where environmental conditions are complex can be studied with the in-situ condition to get better results as compared with laboratory tests [12]. Water hardness containing calcite and calcium has been consistently observed forming corrosion on the wall of the pipe that is exposed to water that has high hardness [13].

Several sorts of studies have been done in numerous countries throughout the world, including the National Science Foundation (USA), the Australian Research Council (Australia), the Engineering and Physical Sciences Research Council (UK), and the National Research Council (Canada) [14]. This demonstrates that the influence of corrosion on buried metallic structures remains an active research topic, as managing corrosion risk is challenging due to a wide range of environmental and material corrosiveness. The mechanisms of internal corrosion damage become dominant over the pipelines as the service years increase with the combined effects of environmental, material, and corrosion attack. The influences of water pipeline failure mechanisms are broadly classified into two categories: (1) structural deterioration that is unable to withstand stresses acting on it, and (2) the slow reduction of pipe wall caused by corrosion and water pressure degrades structural capacity and water quality. Water pipe corrosion damage mechanisms are related to soil condition [15, 16], microorganisms [17], and water quality parameters [3].

Pitting corrosion is the main problem of water pipes which damages localized pipe surfaces. It has a progressive damaging process including pitting initiation, propagation, and termination that go through until leakage formation. During the initiation stage, the film cracks at first condition due to a variety of causes such as pipe and environment interaction, non-homogeneity in the corrosion scale, and the presence of chloride and fluoride. When the films break, a stagnant water condition can cause localized pitting on the pipe's surface due to deposits. Furthermore, oxygen, and water moisture combine to generate electrochemical reactions at the cathode, forming hydroxide ions, and at the anode, causing metal dissolution Eqns. 1 and 2.

$$H_2O + O_2 + 4e^- \rightarrow 4OH^- \quad (1)$$

$$Fe + 2e^- \rightarrow Fe^{2+} \quad (2)$$

This study aims to investigate internal corrosion mechanisms and to characterize their effects on the pipe wall. The results obtained from this study have various useful applicable information for the industries and water distribution system owners to keep water quality, predict the lifetime of buried materials, apply planned pipe maintenance and replacement activities, and corrosion control.

MATERIALS AND METHODS

Sample collection and preparation

Five in-situ condition corrosion damage (CD) of 100 mm diameter galvanized steel (GS) samples that had been in service for more than 15–20 years and four 350 mm diameter ductile cast iron (DCI) water mains samples served for more than 30 years were collected from Addis Ababa city's water distribution systems (WDS) for corrosion characterization. In addition, new pipe samples were prepared for microstructural study from each type of pipe Table 1.

The coating thicknesses of DCI and GS pipes were 25 and 55 μm respectively. The pipe's elemental compositions of galvanized steel and ductile cast iron were determined using a spark

Table 1. The number of pipe samples and methods used

Sample type	Number of samples	Testing method
Ductile cast iron	Corroded pipe: 4	• Surface analysis software (Mountains) • Water laboratory test. • SEM, OM
	New pipe: 1	
Galvanized steel pipe	Corroded pipe: 5	
	New pipe: 1	

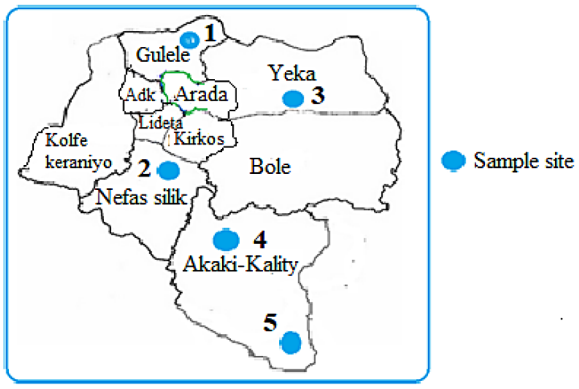

Fig. 1. Sites of water samples and iron pipes collected in the municipal

spectrometer. The samples were dust-free after being cleaned with a cotton cloth and ground with silicon carbide abrasive paper. Then the spectrometer (of Oxford Instruments PMI-Master Smart, Germany) was calibrated. To eliminate the possibility of inaccuracy, each sample surface was tested (burned) three times at different locations to obtain average reading values, as shown in Tables 2 and 3, respectively. Meanwhile, five water samples were collected from the same locations for the analysis of internal corrosion factors from water quality Fig. 1.

Figures 2a and b show internal corrosion patterns of ductile cast iron and galvanized pipes respectively. Compared to the two pipes, more corrosion damage was observed on the galvanized pipe wall. In addition, corrosion scale and localized pitting corrosion were detected visually at the macro level.

Image processing

Mountains 9 digital surface analysis software; Digital Surf, France was used to characterize corrosion morphology and pitting features. The software detects the images situation based on the method of threshold segmentation of ISO 25178-2 [18] watershed standard to determine corrosion characteristics from the sources of SEM images.

Test of water physicochemical

Water parameters were tested using laboratory equipment such as the Miero 800, Burete Lab pH 7310p, DR 900, and Palin test Photometer

Table 2. Elemental compositions of galvanized steel pipe

Elements by wt.%										
C	Mn	Si	Ni	P	Mo	Cr	S	V	Al	Fe
0.087	0.41	0.117	0.06	0.01	0.01	0.10	0.01	0.09	0.05	Bal.

Table 3. The material composition of ductile iron pipe in wt.%

Parameter	Elements											
Pipe	C	Mn	P	S	Si	Ni.	Cr	Mo	Cu	Ti	Mg	Fe
DIP	3.600	0.340	0.090	0.032	2.250	0.060	0.070	0.001	0.080	0.14	0.008	Balance

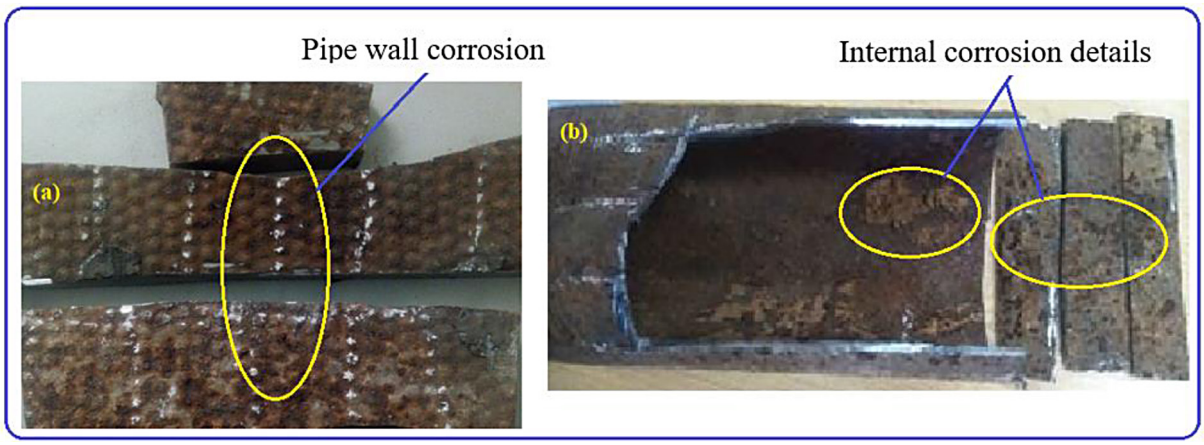

Fig. 2. Photographs of internal pipe corrosion morphology: (a) Ductile cast iron pipe and (b) Galvanized steel pipe

7100 (Germany 2018) for detecting conductivity, total hardness, water pH, chlorine dioxide, and released iron test were used to identify major causes of internal pipe corrosion damage.

Characterizations of pipe materials

New galvanized steel (GS) and ductile cat iron (DCI) pipe materials were prepared for the characterization of microstructures. Optical microscopy (OM, Huvitz HR-300 series, Huvitz, Gunpo, Korea) was used to analyze the microstructures and whether defects are available or not during the manufacturing process that can contribute to corrosion. Sample preparation procedures were done following the procedures including cutting, mounting and grinding using different sizes of emery paper grit numbers including 400, 800, 1200, and 2000. The pipe specimens were then polished with a grit of 6-micrometer disc before being etched into the solution of ethanol 50 ml and 1% of HNO_3 for 3 seconds to produce a mirrored surface before OM analysis. Additionally, corroded water pipe samples were prepared from each type of DCI and GS pipe having 15 mm x 15 mm to study internal pipe corrosion morphology by using SEM JEOL Japan, Kyoto, Japan.

Determining corrosion rate

The mass loss of corroded pipes was evaluated based on the usual corrosion rate calculation model considering buried exposure time (in-situ condition) from the period of pipe installation up to the failure was determined in terms of mass loss per unit area Eqn. 3.

$$C_{rate} = \frac{\mathrm{K}.\Delta \mathrm{W}}{A\rho t} \tag{3}$$

where: ΔW is mass change and C_{rate} is the rate of corrosion are in g and mm/y, respectively; A is the corroded surface area in cm^2; t is buried time in hours; K = 8.76 x 10^4 is a constant value of error minimization and ρ = 7.86 g/cm^3 is the density of steel pipe.

RESULTS AND DISCUSSION

Analysis of water physicochemical parameters

Internal pipe corrosion is influenced by water physicochemical parameters such as alkalinity, protective film stability, and low pH, as well as the presence of heavy metals in the drinking water, which can induce corrosion and pose a health risk. Similarly, corrosion mechanisms such as dissolved oxygen concentration, erosion-corrosion and corrosion behavior of the pipes were identified as the key internal pipe corrosion damage. The other corrosion mechanism of the pipe wall is the alloying process of pipe manufacturing due to the contact of dissimilar alloying elements which form galvanic corrosion. To mention collectively, the main pipe failure mechanisms are corrosion, the presence of defects during manufacturing, the impact of some water physicochemical, and water flow rate with high pressure. The results of the water physicochemical laboratory test are shown in Table 4. The pH of the water was found to be between 7.05 and 7.86, which is within the standard of WHO range of 6.5 to 8.5 (4th edition, 2011) [19] and has no influence on pipe corrosion. The lower level of ClO_2 (0.0–0.5 ppm), on the other hand, implies that the amount is being highly influenced by pipe wall corrosion.

Chlorine dioxide is used in drinking water as a disinfectant; however, it has a degrading impact on pipe walls [20]. Under the electrochemical process of cathodic and anodic reactions, the release of corrosion products into the water results in a loss of water quality [3]. This is due to the dissolution of iron taking place at the anode (Eqn. 4) and creating pit depth which able to hold chloride and other ions which accelerate the rate of localized corrosion.

$$\mathrm{Fe} \rightarrow \mathrm{Fe}^{2+} + 2\mathrm{e}^- \tag{4}$$

While the cathodic reaction is affected by oxygen:

$$\mathrm{H_2O} + \mathrm{O_2} + 2\mathrm{e}^- = 2\mathrm{OH}^- \tag{5}$$

The presence of inorganic salts and organic matter in the water as microscopic particles are capable of forming deposits on the pipe wall at stagnant condition of water flow indicates the presence of total dissolved solids. As presented in Table 4, the total dissolved solids (TDS) ranged from 84.10 to 262.8 ppm. The highest TDS value was found in sample code #5, which was 262.8 parts per million (ppm). This demonstrates that the number of solid particles in groundwater is higher than the number of solid particles in surface water due to the presence of dissolving substances while water moves in the soil [21]. Though the TDS level was higher than in other samples, it did not affect health,

Table 4. Water physicochemical analysis results

Water parameter	Site codes					WHO (2011)
	#01	#02	#03	#04	#05	
pH	7.71	7.05	7.64	7.68	7.86	6.5–8.5
Chlorine dioxide (ppm)	0.5	0.05	0.0	0.12	0.0	0–0.2
Total hardness ($CaCO_3$) (ppm)	84	87	90	77	215	61–121
Fe^{+3} (ppm)	0.45	0.0	0.1	0.55	0.05	0–0.3
Conductivity of water (µS/Cm)	171	197	197.3	157.8	493.4	up to 400
Total dissolved solids (ppm)	91.6	105	105.4	84.10	262.8	up to 500
Dissolved Oxygen (ppb)	80	-	-	81	80	-

but the solids were able to develop deposits on the pipe wall over time during water stagnant condition and damages pipe surface Fig. 3. Additionally, water electrical conductivity (EC) in Table 4 shows from (157.8–493.4 µS/Cm). The EC depends based on the amount of iron released and total dissolved particles in the water. The presence of EC indicates the potential of water able to pass the flow of electric current from the pipe is being higher which enhances the rate of internal corrosion. Table 4 also presents the lab result of ferric ion (Fe^{3+}) ranging from 0.05–0.55 ppm in the analyses. The result obtained from the site of 02, 03, and 05 indicate the release of ferric oxide is at normal condition whereas sites 01 and 04 observed a higher amount of ferric ion; in turn, which shows the rate of internal pipe corrosion condition enhanced by dissolved oxygen. As the attack of ferric oxide increases, it has great potential to form magnetite (Fe_3O_4) corrosion scale which leads to change in water taste and color. The other factor of internal pipe corrosion is water hardness caused by dissolved calcium irons which form protective scales on the pipe wall. As the size of scale increases during the stagnant condition of water flow, it creates turbulent and develops erosion-corrosion.

During the chemical reaction of iron, oxygen, and water, dissolved oxygen (DO) induces

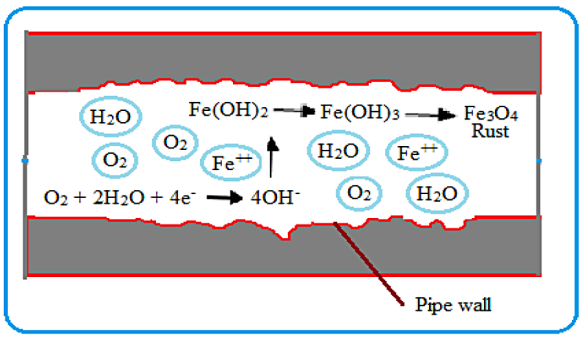

Fig. 3. Schematics of pipe wall corrosion formation process

the formation of iron oxides in the water. Internal pipe wall corrosion is accelerated by DO, which is deoxidized at the cathode during electrochemical processes. DO's laboratory report indicates that the results are in the 80–81 ppb range, indicating that internal corrosion is accelerated and ferrous oxides are formed as a result of chemical reaction:

$$O_2 + 2H_2O + 2Fe \rightarrow 2Fe(OH)_2 \quad (6)$$

$$O_2 + 4Fe + 2H_2O(OH)_2 \rightarrow 4Fe(OH)_3 \quad (7)$$

In general, even though, the concentrations of the drinking water physicochemical are at standard level and have no health effect, some parameters can be the mechanisms such as dissolved oxygen, total dissolved solids, erosion-corrosion, and water pressure are the main actors to damage pipe wall.

Characterization of corrosion morphology

Several SEM photos sizes were taken including (50, 100, 200, 500) µm & 1 mm. For this study, 500 µm is used with a magnification of X50 as shown in the figure below. Figure 4a–c depicts the morphologies of internal corrosion in SEM images. Figure 4a shows the SEM image of the DCI pipe wall which was damaged by the uniform and localized corrosions during the service years with operating water pressure of 150–350 kPa. Similarly, Figure 4b presents the corrosion damaged surface of galvanized pipe. The surface is deteriorated as a result of pitting corrosion growth caused by the deposits, dissolved oxygen, long time water conveying service, and alternating of water pressure. Perforation and tubercles of iron pipes depend on the pipe material, and the variety of corrosion products that affect service lifetime. Similarly, Figure 4c shows the corrosion crystals of GS pipe having irregular shapes and porous textures due to the formation of pitting at random locations which breaks corrosion films.

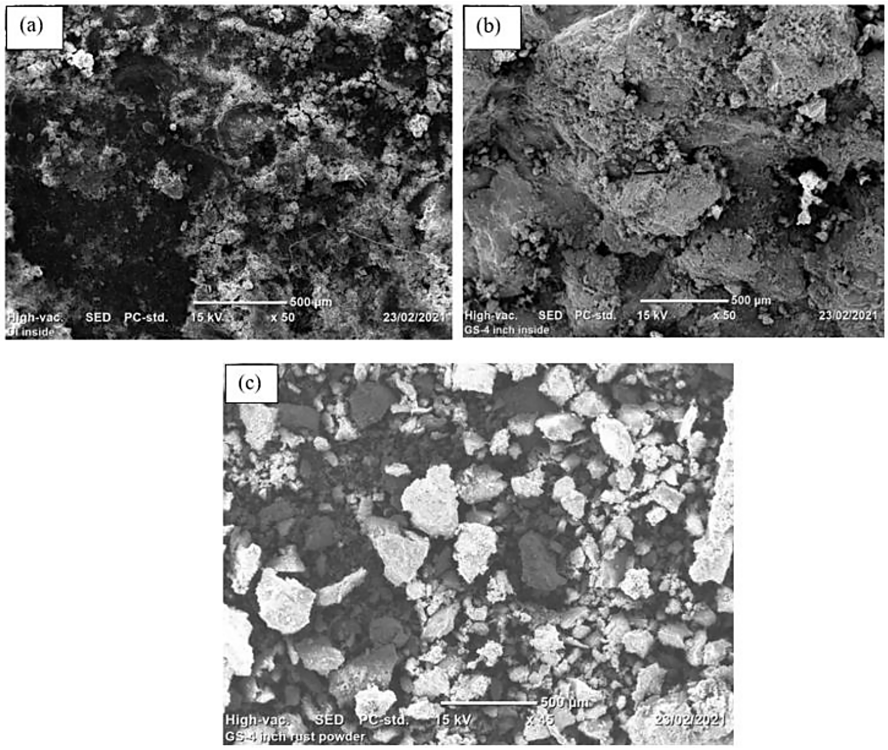

Fig. 4. Micrographs of SEM internal pipe corrosions: (a) ductile iron; (b) Galvanized steel pipe and (c) corrosion crystals of GS pipe

Microstructure analysis

The microstructural analysis is crucial to investigate the presence of defects, inoculants, compositions, and inclusions during manufacture. Figure 5 a–c shows a micrograph of a DCI pipe consisting of black circles of graphite and white pearlite structures. The tendency of pitting and intergranular corrosion occurring on the surface of DCI, according to OM's image analysis, is between the surrounding graphite nodules. Similarly, Figure 5d & e depict the microstructure of

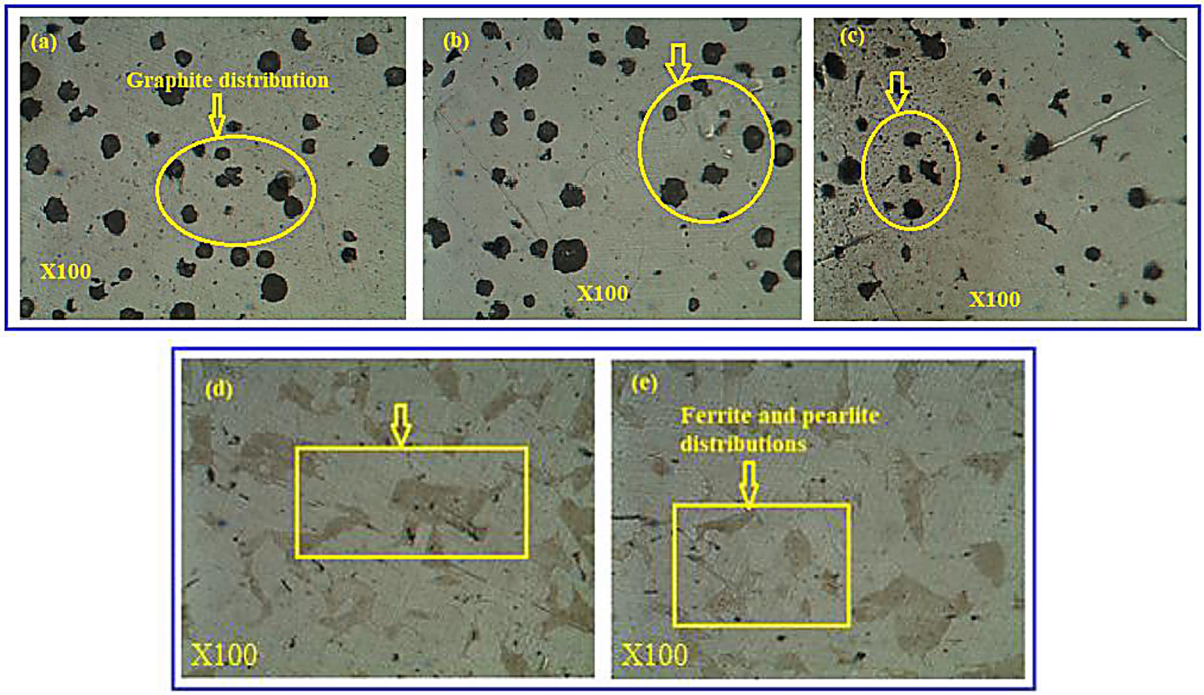

Fig. 5. Microstructures: (a–c) Ductile cast iron and (d and e) Galvanized steel pipe

GS pipe, which consists of white pearlite and gray ferrite structures separated by grain boundaries. The carbon content of the tested galvanized steel was 0.087 wt.% presenting ferrite-pearlite microstructures with dominant ferritic structure. Similarly, the tested pipe sample has 0.117% silicon by weight, which improves the tensile strength of the pipe. The grain size and boundaries of the samples were observed as uniform distributions of alloying elements based on optical microscope (OM) analysis. The OM images of X100 magnification present the patterns and distributions of microstructures of the samples. Different magnification can be used to observe more clearly the internal structures, but in this study, X100 was used to investigate distributions of ferrite-pearlite structures.

Image processing analysis

The Mountain9 software characterizes different corrosion features including pit depth, area, pit form, and volume based on the watershed segmentation. Figure 6a shows the SEM image morphology of corroded galvanized steel pipe, which was used as the source of image processing to determine pit depth, area, and volume using the software. Similarly, Figure 6b depicts the topography of corrosion-degraded pipe surface filled watershed segmentation with particle boundary in pseudo-color of the surface, which is ready for image processing analysis at the particle level. The blue color represents a more damaged localized surface. Similarly, the red color depicts the top layer of the pipe surface which is going to be damaged layer-by-layer.

Figure 7a presents a 3D image of corrosion-damaged topography whereas Figure 7b shows the cross-sectional of the sample having details of pit depth. The image processing results produced from Mountains 9 surface analysis software are shown in Figures 8a and b. The result shows that maximum pit depth equals the sum of the maximum peak (Z-max) and valley (Z-min) values, which is 200 µm

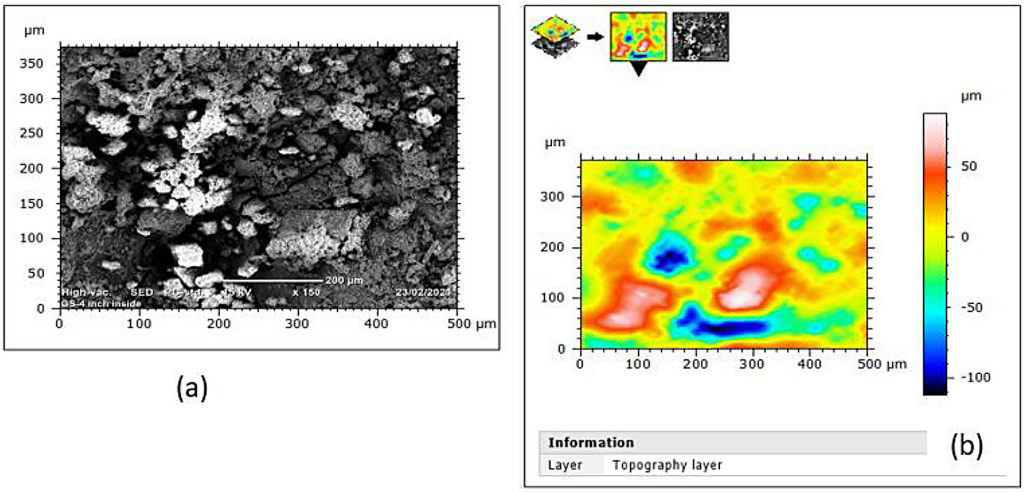

Fig. 6. Image processing: (a) true color of SEM view, (b) topography layers

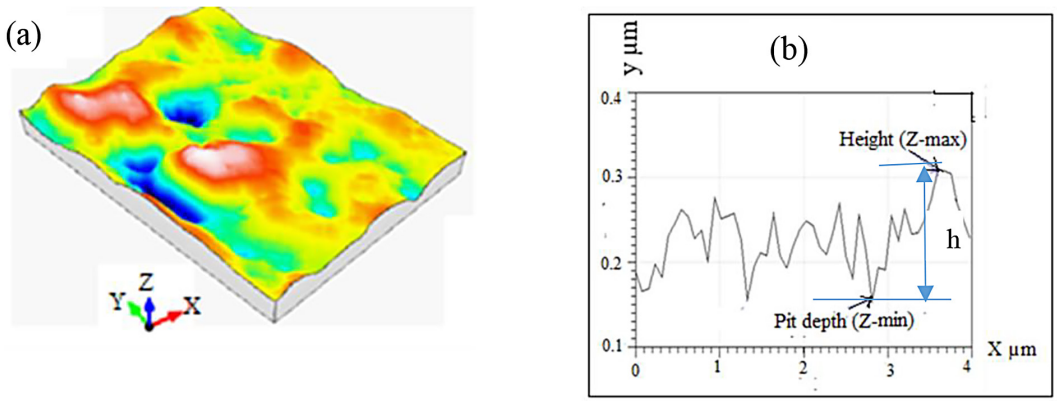

Fig. 7. Corrosion morphology characterization of GS pipe: (a) 3D image of watershed segmentation of corroded surface and (b) cross-section of corrosion damaged surface

after a 30% loss of original pipe thickness of 5 mm Figure 8. The average pit depth that existed on both internal and external surfaces was evaluated using Eqn. 8 to determine the remaining pipe thickness.

$$T_l = T_o - t_r \tag{8}$$

where: T_l is pipe thickness loss, T_o and t_r are original and remained thicknesses of the pipe sample.

Figure 9 shows watershed segmentation of internal pipe corrosion damage which was generated from the SEM image. The entire surface of the sample is filled with watersheds and divided into several particles with their boundaries. This is an important condition of image processing to characterize corrosion-damaged surfaces at the particle level. The Figure shows a corrosion-damaged surface that was filled with watershed and studied at the particle level. The particles are colored automatically and divided by grain boundaries. The surface colored with blue, red, and yellow represent the decreasing order of corrosion damage. This method of corrosion characterization is used for determining the state of corrosion on metallic materials at any given time and aids to make decisions to apply corrosion-prevention strategies.

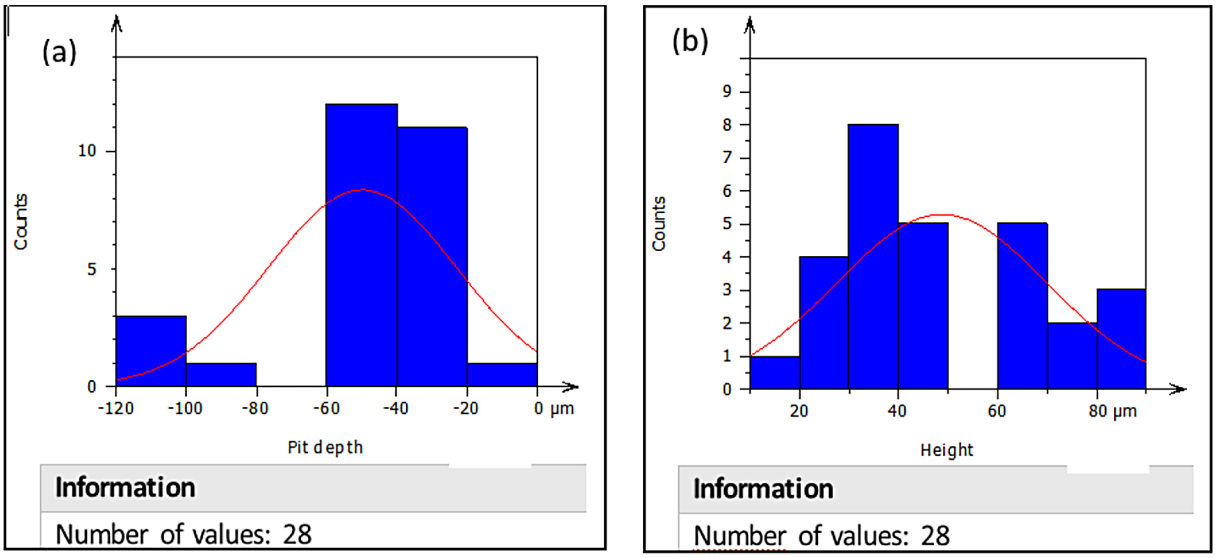

Fig. 8. Result of image processing: (a) pit depth, (b) height (Z-max)

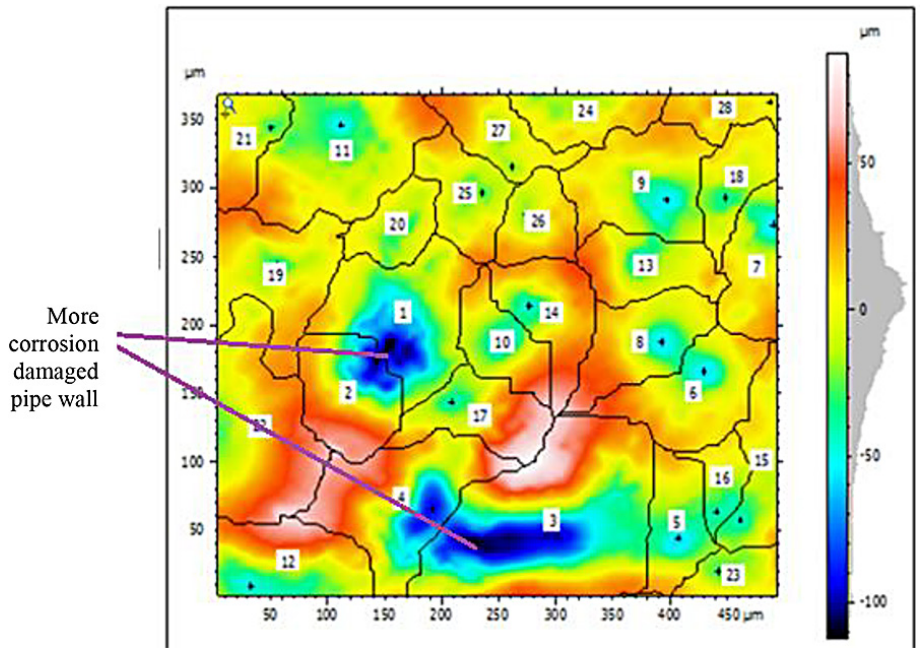

Fig. 9. Watershed segmentation of corrosion damaged GS pipe surface

The SEM image was automatically divided by the software into several particles for detailed analyses of corrosion at the particle level. Based on the image processing result, maximum pitting corrosion area and volume are (43164 μm²) and (182845 μm³) respectively reported as the rate of corrosion as shown in Figure 10 at particle #1.

Figures 11 to 14 present corrosion characterizations of ductile cast iron using image processing to investigate corrosion morphology and pitting characteristics. Figure 11a is the SEM image source of the sample with its true color and Figure 11b depicts the topography of corrosion damaged surface filled by watershed and the status of corrosion damaged surface is isolated by different colors to show that the sample is ready for corrosion characterization. Similarly, Figure 12a shows the 3D form of the watershed surface which describes the loss of the pipe thickness while Figure 12b presents the cross-sectional details of the sample to demonstrate the depth of pit and maximum height remaining on the pipe surface. Figure 13 and 14 also show that the results obtained from image processing in the form of table and bar graphs respectively. The particle analysis of watershed segmentation

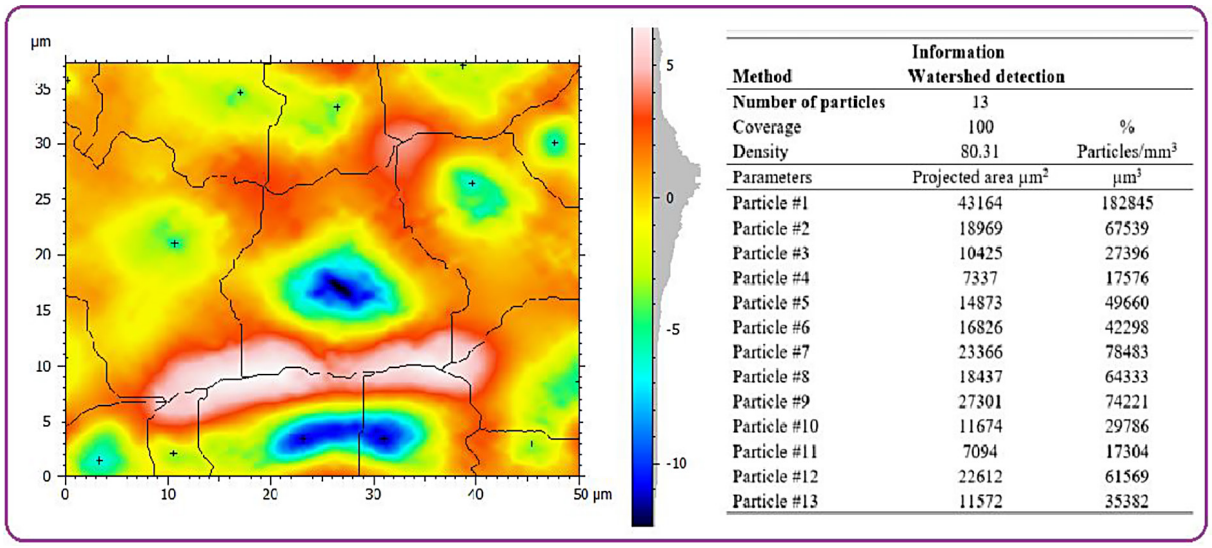

Information		
Method	**Watershed detection**	
Number of particles	13	
Coverage	100	%
Density	80.31	Particles/mm³
Parameters	Projected area μm²	μm³
Particle #1	43164	182845
Particle #2	18969	67539
Particle #3	10425	27396
Particle #4	7337	17576
Particle #5	14873	49660
Particle #6	16826	42298
Particle #7	23366	78483
Particle #8	18437	64333
Particle #9	27301	74221
Particle #10	11674	29786
Particle #11	7094	17304
Particle #12	22612	61569
Particle #13	11572	35382

Fig. 10. Corrosion pit area and volume per particle (GS) pipe

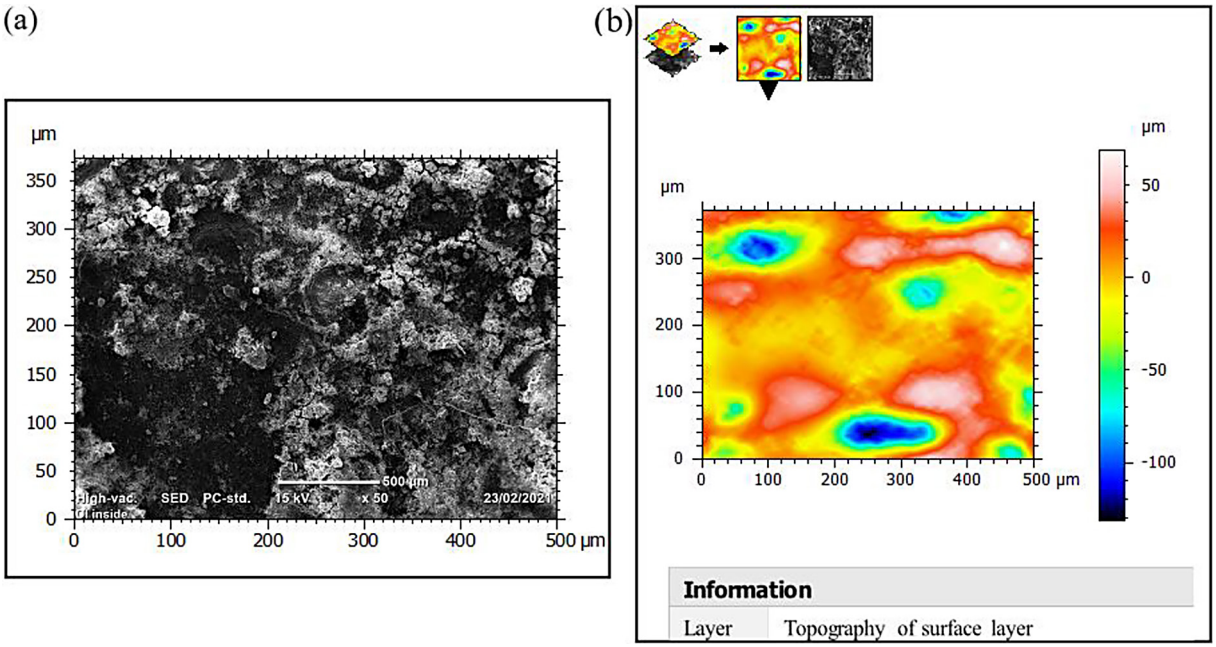

Fig. 11. Corrosion characterization of DCI: (a) true color of SEM view, (b) topography layers

describes the threshold condition of pitting features. The depth of corrosion is 190 µm which is the threshold value after a 30% thickness loss of 8 mm original thickness.

Analysis of internal corrosion damage

Identifying corrosion damage mechanisms, corrosion control, water quality, and prediction of

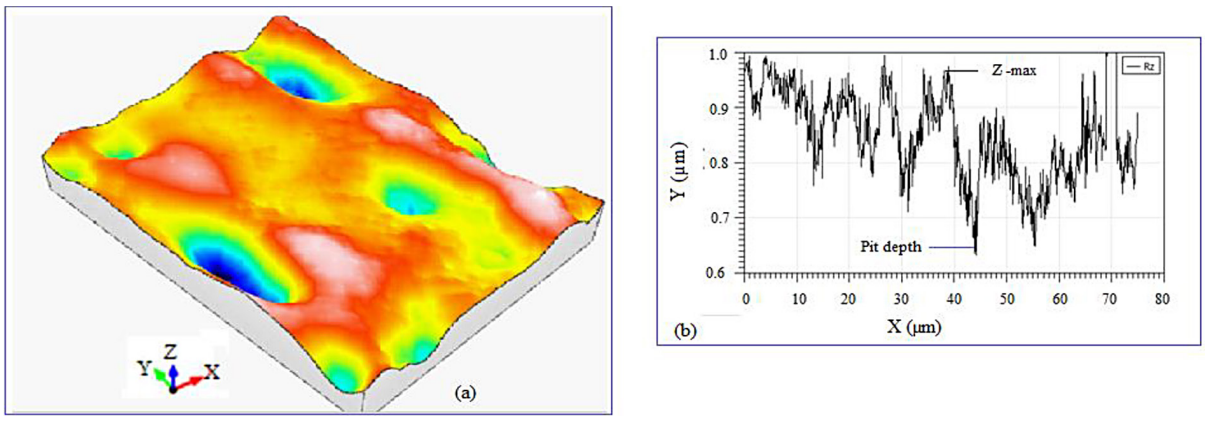

Fig. 12. Corrosion morphology analysis of DCI: (a) 3D image of watershed segmentation of corroded surface and (b) cross-section of corrosion damaged surface

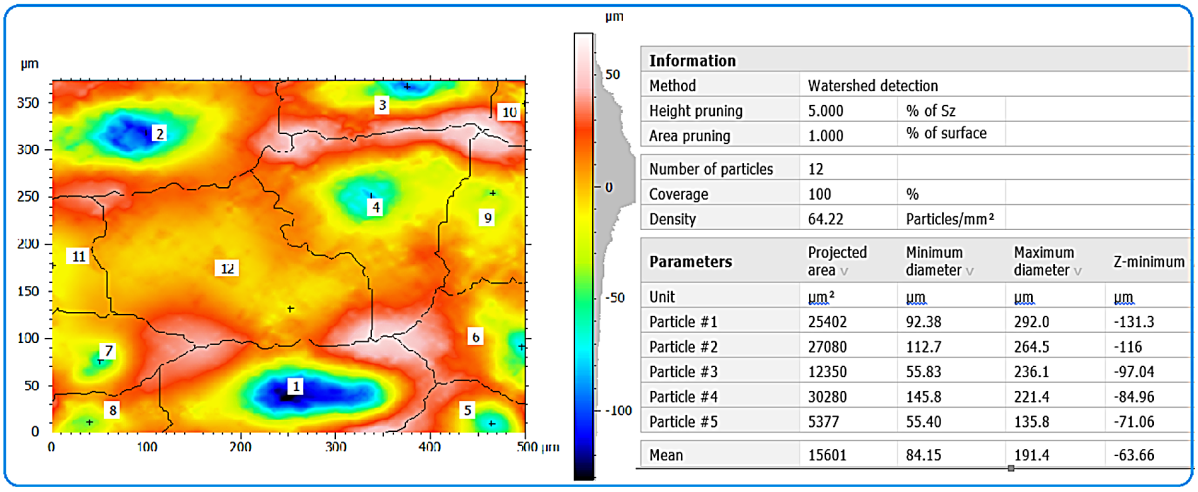

Fig. 13. Watershed segmentation of corrosion showing pit area and depth per particle (DCI)

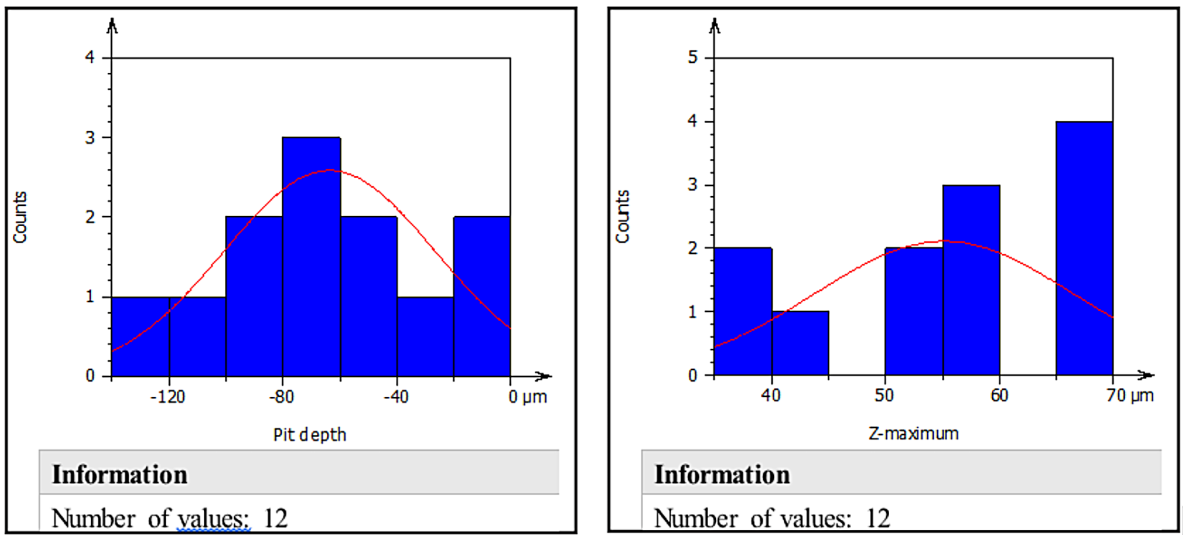

Fig. 14. Result of image processing (a) Pit depth, (b) Height

the remaining pipe age are major concerns of water supply owners. The characteristics of corrosion damage depend on the condition of corrosion films or scales. Many factors, including water pipe materials and manufacturing processes, bacteria, water treatment chemicals, dissolved oxygen, and a lack of planned inspection and maintenance, all contribute to the buried water pipelines corrosion damage. Additionally, Dissolved gases such as oxygen and carbon dioxide in water transport are other origins of internal pipe wall corrosion mechanisms [22]. Other internal corrosion elements in the working environment, such as water velocity and pressure, have a major role in the creation of erosion-corrosion and stress corrosion cracking over service time. Water flow categorized as low velocity (0.07 m/s), medium velocity (0.4–0.6 m/s), and high velocity (approximately 1.5–2 m/s) [2]. Water velocity data were used to evaluate the condition of erosion-corrosion. When the velocity is higher, erosion-corrosion develops with the help of pipe service load. As the progress of corrosion damage increases, water flow creates turbulent and damaged pipe walls. On the other hand, during the stagnant condition of water flow, the bottom part of the pipe wall has more damage than other surfaces due to deposits lying on the surface. Pipe damage symptoms such as localized pitting size, pipe wall fracture, and surface deterioration are critical characteristics to consider while doing pipe maintenance [23, 24].

The rate of corrosion was determined from a typical 15 year old GS pipe was determined based on the weight loss method. Using Eqn. 3, inserting the values of constant ($K = 8.76 \cdot 10^4$, (ΔW = 160 g, D = 2.54 cm, $A = 2\pi Dh = 160$ cm^2, and h = 10 cm, $\rho = 7.86$ g/cm^3 and t = 131400 hrs. estimated for 15 years) in the equation, the computation gives 0.084 mm per year. This corrosion rate value indicates the reduction of pipe weight, and which confirms the deterioration of pipe structure due to water physicochemical parameters, and soil corrosivity during the service year.

In general, the rate of corrosion damage depends on the variety of mechanisms including water physicochemical forming oxidation and reduction process on the pipe wall, soil environment, erosion-corrosion, stress corrosion cracking, and the combined effect of these mechanisms. Once buried ferrous materials are corroded, characterizations are very important to understand corrosion behaviors from the viewpoints of water parameters and environmental impacts for the application of corrosion prevention methods. Chemical additions such as a little amount of sodium bicarbonate during water treatment, as per WHO standards, are highly helpful for controlling internal pipe corrosion (IPC). Using digital image and field survey, as compared to the IPC with external pipe corrosion (EPC) damage, pipe wall corrosion is more affected than external corrosion. More corrosion-damaged locations were observed at the bottom of the pipe on both inside and outside surfaces. Based on the analysis of water physicochemical, site #5 is more corrosive to the pipe wall. Similarly, the rate of metal dissolution in galvanized steel pipe is higher than ductile cast iron pipe, according to pitting corrosion characterization using the software. For pipeline safety and water quality, periodic pipe washing and in-line inspection, as well as annual pipe servicing, are critical to controlling internal pipe corrosion.

CONCLUSIONS

Internal pipe corrosion damage mechanisms (CDMs) were studied on the DCI and GS water pipes and corrosion characterization was performed to investigate corrosion behaviors. Major CDMs were identified including electrochemical corrosion, operation conditions, water physicochemical, and defects from pipe manufacturing.

Based on the study conducted on the internal corrosion damage mechanisms of buried ductile cast iron and galvanized water pipes, the following conclusions can be drawn. The water physicochemical analysis shows that the main mechanisms of the internal pipe wall are dissolved oxygen, chlorine dioxide, total dissolved solids and total hardness. Corrosion characterization using a scanning electron microscope was done to evaluate corrosion morphology and crystals. Based on the study, micro-cracks and perforation are developed from the subsurface of the pipes. Water pH has no significant effects on corrosion formation and conductivity insists on corrosion cell formation. Based on weight loss calculation, the rate of corrosion on the buried galvanized pipe of 0.042 mm/y is obtained in the loam soil. The microstructural analysis, though the samples have uniform structural distribution, indicates that galvanic corrosion is formed due to dissimilar structures (ferrite-pearlite) contacting each other in the case of galvanized steel. Similarly, intergranular corrosion forms between the contact of grain boundaries and the structures between graphite of ductile cast iron and pearlite.

In summary, internal corrosion is a complicated process caused by a range of corrosion mechanisms including pipe material manufacturing, electrochemical corrosion, and operational conditions. To manage corrosion mechanisms, water supply owners must conduct frequent inspections, maintain historical pipe data, test water quality after treatment, wash pipelines on a regular basis, and do preventative maintenance.

Acknowledgments

The authors would like to thank Adama Science and Technology University (ASTU) and Addis Ababa Water and Sewerage Authority (AAWSA) for their cooperativeness.

REFERENCES

1. Mahmoodian M., Aryai V. Structural failure assessment of buried steel water pipes subject to corrosive environment. Urban Water Journal. 2017; 14: 1–8. DOI: 10.1080/1573062X.2017.1325500
2. Treesa B., Jaspreeth N., Ranjith S.K., Jiji C.V., NDT and E international visual inspection and characterization of external corrosion in pipelines using deep neural network. NDT and E International. 2019; 107: 102134. DOI: 10.1016/j.ndteint.2019.102134
3. Hu J., Dong H., Ling W., Qu J., Qiang Z. Impacts of water quality on the corrosion of cast iron pipes for water distribution and proposed source water switching strategy. Water Research. 2017; 129: 428–435. DOI: 10.1016/j.watres.2017.10.065
4. Sanjuan-Delmás D., et al. Environmental assessment of different pipelines for drinking water transport and distribution network in small to medium cities : a case from Betanzos, Spain. Journal of Cleaner Production. 2014; 66: 588–598. DOI: 10.1016/j.jclepro.2013.10.055
5. Sun H., Shi B., Yang F., Wang D. Effects of sulfate on heavy metal release from iron corrosion scales in drinking water distribution system. Water Research. 2017; 114: 69–77. DOI: 10.1016/j.watres.2017.02.021
6. Li M., Liu Z., Chen Y., Hai Y. Characteristics of iron corrosion scales and water quality variations in drinking water distribution systems of different pipe materials. Water Research. 2016; 106: 593–603. DOI: 10.1016/j.watres.2016.10.044
7. Cui J., Wang D., Ma N. Case studies on the probabilistic characteristics of ultimate strength of stiffened panels with uniform and non-uniform localized corrosion subjected to uniaxial and biaxial thrust. International Journal of Naval Architecture and Ocean Engineering. 2018; 11(1): 97–118. DOI: 10.1016/j.ijnaoe.2018.02.011
8. Hou Y., Lei D., Li S., Yang W., Li C. Experimental investigation on corrosion effect on mechanical properties of buried metal pipes. International Journal of Corrosion. 2016; 5808372. DOI: 10.1155/2016/5808372
9. Vanaei H.R., Eslami A., Egbewande A. A review on pipeline corrosion, in-line inspection (ILI), and corrosion growth rate models. International Journal of Pressure Vessels and Piping. 2017; 149: 43–54. DOI: 10.1016/j.ijpvp.2016.11.007
10. García-mora B., Debón A., Santamaría C., Carrión A. Modelling the failure risk for water supply networks with interval-censored data. Reliability Engineering and System Safety. 2015; 144: 311–318. DOI: 10.1016/j.ress.2015.08.003
11. Shuai Y., Shuai J., Xu K. Probabilistic analysis of corroded pipelines based on a new failure pressure model. Engineering Failure Analysis. 2017; 81: 216–233. DOI: 10.1016/j.engfailanal.2017.06.050
12. Lee H., Rasheed U., Kong M. A study on the comparison of corrosion in water supply pipes due to tap water (TW) and reclaimed water (RW). Water. 2018; 10(4): 496. DOI: 10.3390/w10040496
13. Zakowski K., Darowicki K., et al. Case studies in construction materials electrolytic corrosion of water pipeline system in the remote distance from stray currents – Case study. Case Studies in Construction Materials. 2016; 4: 116–124. DOI: 10.1016/j.cscm.2016.03.002
14. Noble F., Stief P., Dantan J., Etienne A., Siadat A. Prediction of corroded pipeline performance based on dynamic reliability models. Procedia CIRP. 2019; 80: 518–523, 2019. DOI: 10.1016/j.procir.2019.01.093
15. Wasim M., Li C., Robert D.J., Mahmoodian M., Setunge S. Experimental investigation of factors influencing external corrosion of buried pipes. Fourth International Conference on Sustainable Construction Materials and Technologies, Las Vegas, USA 2016.
16. Wasim M., Shoaib S., Inamuddin N.M.M., Asiri A.M. Factors influencing corrosion of metal pipes in soils. Environtal Chemistry Letters. 2018; 16: 861–87989. DOI: 10.1007/s10311-018-0731-x
17. Liu D., Jin J., Liang S., Zhang J. Characteristics of water quality and bacterial communities in three water supply pipelines. Royal Society of Chemistry. 2019; 7: 3504–4091. DOI: 10.1039/c8ra08645a
18. ISO 25178-2 Geometrical product specifications (GPS) — Surface texture: Areal — Part 2: Terms, definitions and surface texture parameters, 2012, https://www.iso.org/standard/42785.html.
19. World Health Organization, Guidelines for Drinking-water Quality. 4th Ed. 2011.

20. Shams D.F., Islam S., et al. Characteristics of pipe corrosion scales in untreated water distribution system and effect on water quality in Peshawar, Pakistan. Environmental Science and Pollution Research. 2019; 26: 5794–5803. DOI: 10.1007/s11356-018-04099-6
21. Alamineh E.A. Study of iron pipe corrosion for water distribution system and its effect in Addis Ababa City; Ethiopia. American Journal of Environmental Sciences. 2018. DOI: 10.3844/ajessp.2018
22. Vertova A., Miani and et al. Chlorine dioxide degradation issues on metal and plastic water pipes tested in parallel in a semi-closed system. Environmental Research and Public Health. 2019; 16(22): 4582. DOI: 10.3390/ijerph16224582
23. Chowdhury R.R., Alam M.M., Islam A.K.M.S. Numerical modeling of turbulent flow through bend pipes. Mechanical Engineering Research Journal. 2017; 10: 14–19.
24. Shin S., Lee G., Ahmed U., Lee Y., Na J., Han C. Risk-based underground pipeline safety management considering corrosion effect. Journal of Hazardous Materials. 2018; 342: 279–289. DOI: 10.1016/j.jhazmat.2017.08.029